RESEARCH ARTICLE | AUGUST 27 2001

Dissociation of grain boundary dislocations in $SrBi_2Ta_2O_9$ ferroelectric thin films

Xinhua Zhu; Jianmin Zhu; Shunhua Zhou; Qi Li; Zhiguo Liu; Naiben Ming

Appl. Phys. Lett. 79, 1345–1347 (2001)
https://doi.org/10.1063/1.1388866

Dissociation of grain boundary dislocations in $SrBi_2Ta_2O_9$ ferroelectric thin films

Xinhua Zhu,[a] Jianmin Zhu, Shunhua Zhou, Qi Li, Zhiguo Liu, and Naiben Ming
National Laboratory of Solid State Microstructures, Department of Physics, Nanjing University, Nanjing 210093, People's Republic of China

(Received 6 April 2001; accepted for publication 6 June 2001)

In this work, the dissociation of grain boundary dislocations (GBDs) is reported in $SrBi_2Ta_2O_9$ (SBT) ferroelectric thin films with *c*-axis orientation grown by pulsed-laser deposition on $Pt/TiO_2/SiO_2/Si(100)$ substrates. Small-angle (8.2°) [001] tilt grain boundaries with a boundary plane close to the (110) plane exhibit partial GBDs separated by stacking faults. The dissociated grain-boundary structures have twice the number of GBDs and interdislocation core channel width smaller than that Frank's geometrical rule predicts. At the equilibrium, the repulsive elastic force between partial dislocations is balanced by an attractive force produced by the formation of a stacking fault between the partials. Based on this, the stacking fault energy is evaluated to be 0.27–0.29 J/m^2. The relationship between the leakage current of SBT films and dissociation of GBDs is also discussed. © *2001 American Institute of Physics.* [DOI: 10.1063/1.1388866]

Ferroelectric thin films are interesting topics of current researches both under applied and fundamental aspects. $Pb(Zr, Ti)O_3$ (PZT) and $SrBi_2Ta_2O_9$ (SBT) thin films have been used in commercial products, and SBT thin films are particularly promising as the functional elements in ferroelectric random access memories (FeRAMs).[1,2] SBT films are advantageous over PZT films in that they do not suffer from fatigue, whereas PZT films show considerable fatigue if used together with a metallic electrode. Such an advantage of SBT films is due to a consequence of the unique crystal structure of bismuth-layered perovskites. The preparation and physical properties of SBT films have been thoroughly investigated with an emphasis on the applications in FeRAMs. However, the microstructural features such as lattice defects in SBT films are still not well known. There are only very few reports on the lattice defects in SBT films,[3–5] the microstructures of grain boundaries, and grain boundary dislocations (GBDs) are not well understood at the atomic level. Grain boundaries in polycrystalline ferroelectric thin films with fine grain sizes are the main crystal imperfections. They play an important role in determining the leakage–current characteristics and transport properties of materials through the interactions with free charges carriers, intrinsic crystal defects, and impurities.[6] How to control them is one of the most important subjects in developing FeRAMs. In the present study, we report a high-resolution transmission electron microscopy (HRTEM) observation on the grain boundary structures of SBT films with (001)-orientation grown by pulsed-laser deposition. The dissociation of small-angle GBDs was presented. The small-angle (8.2°) [001] tilt grain boundaries with a grain boundary plane close to (110) plane exhibit partial GBDs separated by stacking faults. Here, the stacking fault energy in SBT thin film is evaluated based on the theory of interactions between partial dislocations, and the relationship between the leakage current of SBT films and dissociation of GBDs is also discussed.

SBT films were prepared on $Pt/TiO_2/SiO_2/Si(100)$ substrates by using pulsed-laser deposition.[7] The crystal structures of the films were examined by x-ray diffraction. Transmission electron microscopy (TEM) samples were prepared by a combination of mechanical thinning, dimpling, and ion milling. The microstructures of SBT grain boundaries were examined at the atomic level by HRTEM (JEOL TEM-4000EX) operated at 400 kV with point-to-point resolution of 0.19 nm.

The SBT films were shown be (001) oriented with *c*-axis oriented grains. The grains are polyhedral shapes and have an average size of about 50 nm in length and 35 nm in width. As estimated from the {110} twin contrast, the grain boundaries are predominately low angle ones, with misorientation angles of 10° or less. A detailed account of the microstructural characterization was reported elsewhere.[8] A HRTEM view of a small angle (8.2°) tilt grain boundary with the boundary plane close to the {110} plane of both grains neighboring the boundary is shown in Fig. 1(a). When viewing from the *c* axis, the two grains are related by a small rotation θ about the *c* axis. The strain contrast from the periodic dislocation array is clearly visible in the image, as indicated by arrowheads. The dislocation configuration is illustrated by a corresponding Fourier-filtered image, as shown in Fig. 1(b), which appears with eight segments with nearly equal spacing. The average dislocation spacing was measured to be about 2.7 nm, and the tilt angle θ was about 8.2°, as indicated in Fig. 1(a). In the SBT films with pseudo tetragonal structure, the lattice parameter *a* ($a=0.5531$ nm) is almost equal to that of *b* ($b=0.5534$ nm), whereas *c* ($c=2.498$ nm)[9] is much larger than *a*. Thus, according to the Frank criterion, only those unit dislocations with Burger's vectors of $\langle 100\rangle a$ or $\langle 110\rangle a$ are stable because the large value of the *c* lattice parameter causes the introduction of a unit *c* com-

[a]Present address: Department of Applied Physics and Materials Research Centre, The Hong Kong Polytechnic University, Hung Hom, Kowloon, Hong Kong; electronic mail: apxhzhu@polyu.edu.hk

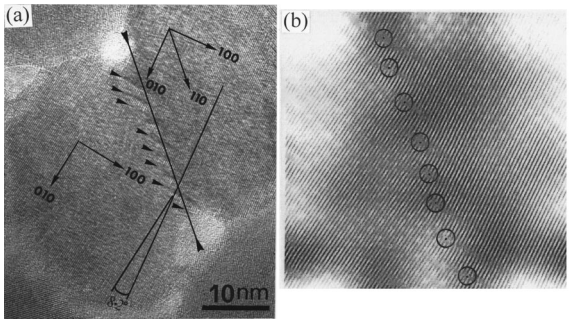

FIG. 1. (a) A HRTEM image of a [001] small-angle (8.2°) tilt grain boundary with near-(110) grain boundary plane. The dislocation contrast of an array of dislocations with an average spacing of 2.7 nm is observed, as indicated by arrowheads and (b) a corresponding Fourier-filtered image of the small-angle tilt grain boundary are shown. Dislocation cores are marked by circles.

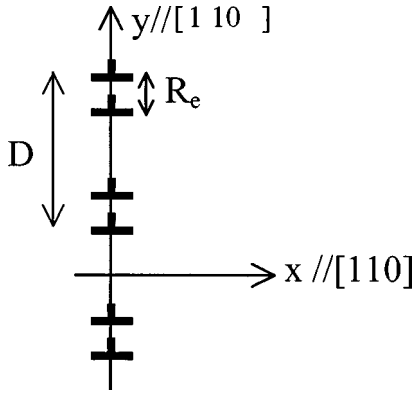

FIG. 2. Schematic diagram for a small-angle pure tilt grain boundary composing of edge-dislocation array with Burger's vector $\mathbf{b}=\frac{a}{2}[110]$ parallel to the x axis, in which D is the total dislocation spacing and R is the separation distance between the partials.

ponent into the Burger's vectors to be highly unfavorable from the viewpoint of energetic minimization. The calculated spacing for the unit edge dislocation with Burger's vector $\mathbf{b}=\langle 110\rangle a$ would be 5.56 nm, which is twice the measured spacing of the GBDs. Since the strain energy of a dislocation is roughly proportional to b^2, unit dislocations with high strain energy would prefer to dissociate it into two partial dislocations with smaller Burger's vectors as follows:

$$a\langle 110\rangle \rightarrow \frac{a}{2}\langle 110\rangle + \frac{a}{2}\langle 110\rangle + \mathrm{SF}, \tag{1}$$

where SF indicates a stacking fault. Reaction (1) results in a half reduction in the strain energy of dislocation, which is an energetically favorable procedure when assuming that the strain energy of a dislocation goes as b^2. The assignment of the paired dislocations with Burger's vectors $\mathbf{b}=\frac{a}{2}[110]$ is in excellent agreement with the measured dislocation spacing and the tilt angle. This Burger's vector is also consistent with the results of $\mathbf{g}\cdot\mathbf{b}$ invisibility experiment.

Because the (repulsive) elastic force between the partial dislocations is balanced by the formation of a stacking fault between the partials, one can use the equilibrium separation of the partials to estimate the energy of the stacking fault. As depicted in Fig. 2, the small-tilt grain boundary is composed of edge-dislocation array with Burger's vector $\mathbf{b}=\frac{a}{2}[110]$ parallel to the x axis, in which D is the total dislocation spacing and R is the separation distance between the partials.

At the equilibrium separation $R=R_e$, the repulsive force per unit length (F_{rep}) between a pair of $\frac{a}{2}\langle 110\rangle$ partial edge dislocations, should be equal and opposite to the attractive force produced by the formation of a stacking fault energy (γ_{sf}), so that the equilibrium condition is[10]

$$\gamma_{\mathrm{sf}}=F_{\mathrm{res}}=-\sigma_{xx}b_x=\frac{\mu b_x^2 \sin\left(\frac{2\pi y}{D}\right)\left[\cosh\left(\frac{2\pi x}{D}\right)-\cos\left(\frac{2\pi y}{D}\right)+2\pi\frac{x}{D}\sinh\left(\frac{2\pi x}{D}\right)\right]}{2D(1-\nu)\left[\cosh\left(\frac{2\pi x}{D}\right)-\cos\left(\frac{2\pi y}{D}\right)\right]^2}. \tag{2}$$

where σ_{xx}, the stress component for the grain boundary, is a summary of contributions from all the individual dislocations in small-angle tilt boundaries, μ is shear modulus, and ν is the Poisson's ratio. Substituting $x=0$ and $y=R_e$ into Eq. (2), the expression of γ_{sf} is given by

$$\gamma_{\mathrm{sf}}=\frac{\mu b_x^2}{2(1-\nu)D}\cot\left(\frac{\pi R_e}{D}\right). \tag{3}$$

Therefore, the stacking-fault energy in SBT films can be calculated by Eq. (3). Because the mechanical data for SBT films are lacking at present, the γ_{sf} value in SBT films is only evaluated by using the corresponding data of SBT ceramics. The Young's modulus of SBT ceramics[11] was reported to be $1.64\times 10^{11}\ \mathrm{N/m^2}$, and the Poisson's ratio for bismuth layer-structured ferroelectric ceramics such as $Bi_4Ti_3O_{12}$, SBT, and $SrBi_4Ti_4O_{15}$ was in the range of 0.23–0.27,[12] therefore, the shear modulus μ for SBT ceramics is calculated to be 64.6–66.7 GPa. For the small-angle tilt grain boundary shown in Fig. 1(a), $R_e=2.7$ nm, $D=6.5$ nm, $\mathrm{Re}/D=0.415$, $b_x=0.39$ nm, the stacking-fault energy γ_{sf} is calculated to be 0.27–0.29 $\mathrm{J/m^2}$, which is only about an half magnitude of stacking faults observed in $YBa_2Cu_3O_{7-\delta}$ superconductor films.[13] Since the magnitude of the stacking-fault energy represents the extent of violation of the proper stacking sequence, it is strongly dependent upon the local bonding nature of grain boundaries in SBT films. In other words, the stacking-fault energy associated with the grain boundary may be used as an indicator of the order parameter for proper stacking, including the oxygen occupancy and mobility. At the small-angle tilt grain boundary, the atoms on each side of the grain boundary have relative $\frac{a}{2}[110]$ translation, as a consequence,

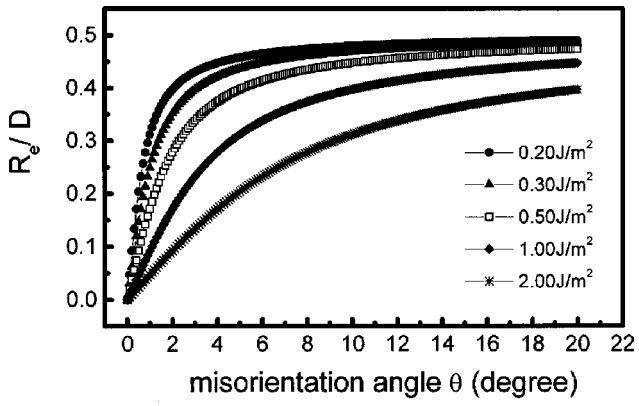

FIG. 3. The relationship between the R_e/D ratio and grain boundary misorientation angle θ as a function of the stacking-fault energy, γ_{sf} is shown. The R_e/D ratio increases as θ increases, and the smaller value the stacking-fault energy, the faster the ratio increases and approaches to 0.5.

the nearby oxygen octahedra form continuous chains in the $a-b$ plane by sharing a face instead of a corner, as found in the perfect SBT. Because of the oxygen octahedra sharing a face with their neighbors at the small tilt grain boundaries, the oxygen occupancy and oxygen octahedra linkage are changed, some oxygen atoms could be saved and some positions of strontium ions could be occupied by tantalum ones.

The measured room temperature leakage–current density (J)-electric field (E) dependence of the films revealed a space charge limited conduction mechanism.[8] Such $J-E$ characteristics are ascribed to the natural features of grain boundaries in the present SBT films. The existence of edge dislocations at small-angle tilt grain boundary is deleterious to the leakage current of the SBT films because the edge dislocations cores can provide pinning centers for the defects such as oxygen vacancies in SBT films, resulting in high leakage current and poor fatigue-resistance characteristics. Since the stacking-fault energy in SBT films is only about an half magnitude of that in $YBa_2Cu_3O_{7-\delta}$ superconductor films, the trapping states in SBT films are shallow, and the distributions of them are usually contributed by the grain boundaries through structural and chemical defects. It has been reported that the oxygen vacancies are weakly pinned by the trapping sites at grain boundaries, and are readily relieved from the trapping sites.[14] Therefore, in SBT films with shallow trapping levels, a large fraction of the injected space chares will condense into the traps, only a fraction of the charges drawn into the film by the applied voltage is available to conduct current, whereas in a trap-free films all the space charges are available to participate in the conduction process.

The relationship between the misorientation angle θ and the extent of partial separation, $\frac{R}{D}$, for a given stacking-fault energy value, can be also evaluated. By substituting θ for b_x/D, Eq. (3) can be rewritten as

$$\frac{R_e}{D}=\frac{1}{\pi}a\tan\left[\frac{1}{\gamma_{sf}}\frac{\mu b_x\sin\left(\frac{\theta}{2}\right)}{1-\nu}\right]. \tag{4}$$

By using Eq. (4), the influence of the misorientation angle θ on the R_e/D ratio for different γ_{sf} values can be obtained, as shown in Fig. 3. For the same θ, a smaller γ_{sf} will give a larger R_e/D ratio. Similarly, for a fixed γ_{sf}, as θ increases, the R_e/D ratio also increases. Furthermore, the smaller the stacking-fault energy, the faster the ratio will increase and approach 0.5. That is the case where the length of stacking-fault region is close to the normal region, and the GBD structure appears to be almost equally spaced. The present condition is just such the case, in which the partial dislocations are almost equally spaced with an average spacing of 2.7 nm, and the stacking-fault energy is smaller, therefore, the trapping states in SBT films should be shallow. Otherwise, if the dissociated GBD configuration has two different spacing, in this case, the grain boundaries should contain the higher energy stacking fault regions between the dissociated partial dislocations, which would contribute to the deep trapping states in materials.

In conclusion, this study reports the dissociation of GBDs in (001)-oriented SBT ferroelectric thin films grown by pulsed-laser deposition on $Pt/TiO_2/SiO_2/Si(100)$ substrates. Small-angle (8.2°) [001] tilt grain boundaries with near-(110) plane exhibit partial GBDs separated by stacking faults. The dissociated grain boundary structures have twice the number of GBDs and a shorter interdislocation core channel width than the Frank's geometrical rule predicts. The stacking-fault energy in SBT films is evaluated to be 0.27–0.29 J/m^2, a half magnitude smaller than that in $YBa_2Cu_3O_{7-\delta}$ conductor films. That implies that the trapping states in SBT films are shallow. The relationship between the leakage current of SBT films and dissociation of GBDs is also discussed.

This work is supported by Motorola Semiconductor Products Sector sponsored research. Part of this work is also supported by the National Natural Science Foundation of China (59832050), the opening project of National Laboratory of Solid State Microstructures (M981308), Nanjing University Talent Development Foundation, and a grant for State Key Program for Basic Research of China.

[1] J. F. Scott and C. A. Paz de Araujo, Science **246**, 1400 (1989).
[2] J. F. Scott, Annu. Rev. Mater. Sci. **28**, 79 (1998).
[3] K. Ishikawa, H. Funakubo, K. Saito, T. Suzuki, Y. Nishi, and M. Fujimoto, J. Appl. Phys. **87**, 8018 (2000).
[4] J. Lettieri, M. A. Zurbuchen, Y. Jia, D. G. Schlom, S. K. Streiffer, and M. E. Hawley, Appl. Phys. Lett. **76**, 2937 (2000).
[5] X. H. Zhu, A. D. Li, D. Wu, T. Zhu, Z. G. Liu, and N. B. Ming, Appl. Phys. Lett. **78**, 973 (2001).
[6] H. J. Moller, Prog. Mater. Sci. **35**, 205 (1991).
[7] X. H. Zhu, Y. M. Liu, Z. H. An, T. Zhu, Z. C. Wu, T. Yu, Z. G. Liu, and N. B. Ming, Thin Solid Films **375**, 200 (2000).
[8] X. H. Zhu, T. Zhu, Z. G. Liu, and N. B. Ming, Appl. Phys. A: Mater. Sci. Process. **72**, 503 (2001).
[9] A. D. Rae, J. G. Thompson, and R. L. Withers, Acta Crystallogr., Sect. B: Struct. Sci. **B48**, 418 (1992).
[10] J. P. Hirth and J. Lothe, *Theory of Dislocations* (Krieger, Malabar, Florida, 1982), p. 733.
[11] F. Yan, X. B. Chen, P. Bao, Y. N. Wang, and J. S. Liu, J. Appl. Phys. **87**, 1453 (2000).
[12] Y. H. Xu, *Ferroelectric and Piezoelectric Materials* (Science, Beijing, 1978), p. 357.
[13] Y. Gao, K. L. Merkle, G. Bai, H. L. M. Chang, and D. J. Lam, Ultramicroscopy **37**, 326 (1991).
[14] J. Robertson, C. W. Chen, W. L. Warren, and C. D. Gutleben, Appl. Phys. Lett. **69**, 1704 (1996).